Accelerated Multi-TI Spiral MRI using Compressed Sensing with Temporal Constraints

X. Chen[1], M. Salerno[2,3], F. H. Epstein[2], and C. H. Meyer[1]
[1]Biomedical Engineering, University of Virginia, Charlottesville, VA, United States, [2]Radiology, University of Virginia, Charlottesville, VA, United States, [3]Cardiology, University of Virginia, Charlottesville, VA, United States

Introduction: Previously, studies have shown that spiral MRI is advantageous for Look-Locker and multi-inversion-time (TI) arterial spin labeling (ASL). However, while multi-TI ASL enables the measurement of parameters such as blood volume, mean transit time, and transit delay in addition to blood flow, the acquisition of multi-TI data is also time consuming. We sought to accelerate multi-TI spiral MRI using compressed sensing (CS). Toward this end, we exploited sparsity in time, investigated different sampling patterns, and used the non-uniform fast Fourier transform (NUFFT) to transform data between image space and *k*-space.

Theory: For multi-TI spiral images (ASL source images), signal intensity changes smoothly with TI, exhibiting sparsity in the temporal domain. However, due to effects such as transit delay, the kinetic signal may not be well described by a simple model such as a sum of T1-relaxation curves. For this reason, instead of a model-based CS approach (1), we implemented a general temporal smoothness constraint using finite-difference methods. Also, because a spiral trajectory does not sample *k*-space on the Cartesian grid, we used the NUFFT to transform data between image space and *k*-space (2). Accounting for these factors, we expressed the CS reconstruction problem as: $m = \arg\min_m \left(\| F_{NUFFT}\, m - y \|_2^2 + \lambda \| \nabla_t m \|_1 \right)$, where m is the image, y is the measured *k*-space data on spiral trajectories, F_{NUFFT} is the undersampled NUFFT, ∇_t is the temporal gradient, λ is a weighting factor for the temporal constraints, and $\|\ \|_2$ and $\|\ \|_1$ are the L2 and L1 norms, respectively (4,5). The first term is the residue term, where the NUFFT operator transforms the estimated image to *k*-space data on spiral trajectories to compute the difference from the measured data. The second term is the sparsity term, where the temporal constraint is introduced and evaluated using the L1 norm. The sparsity term drives the estimated image to be temporally smooth in intensity while the residue term maintains the signal fidelity. The balance between terms is adjusted using λ. An approximation is taken to avoid an L1 norm gradient discontinuity around zero (5). A steepest descent method was implemented to solve this optimization problem and m was updated using $m_{i+1} = m_i + \alpha \Delta m$, where α is the iteration step size and

$$\Delta m = \nabla f(m) = 2 F_{NUFFT}^{-1}\left(F_{NUFFT}\, m - y \right) - \lambda \left(\frac{\nabla_t^2 m}{\sqrt{\nabla_t m (\nabla_t m)^* + \varepsilon}} \right).$$

The NUFFT with min-max interpolation minimizes the worst-case approximation error over all signals. An analytical density compensation function (DCF) was used when converting the *k*-space residue term to the image domain to compensate for non-uniform sampling. To correct the image difference after a pair of NUFFT and inverse NUFFT operations, a scaling factor was introduced to the DCF as $\beta = \max\left(F_{NUFFT}^{-1}\left(F_{NUFFT}\, m_p \right) \right)$, where m_p is a 2D image with a Kronecker delta function at the center.

Methods: Fully-sampled spiral Look-Locker MRI of the mouse heart, as described previously (3), was performed at multiple TIs using a 7T ClinScan MRI system (Siemens, Erlangen, Germany), with the following imaging parameters: field of view = 30 x 30 mm^2, pixel size = 0.24 x 0.24 mm^2, number of spiral interleaves = 87, number of inversion times = 50, and time between inversions = 6 s. Two types of undersampling patterns were investigated. The first type (random) selected random interleaves from fully sampled data for each frame, where the total number of interleaves for each frame was determined by the acceleration rate (Fig.1.A). The second type (uniform rotation) used rotations of angularly-uniformly spaced interleaves, where the initial rotation angle was incremented for successive frames (Fig.1.B). The CS algorithm was implemented in MATLAB. For all data sets, 600 iterations were used to reach a steady state. Acceleration rates of 2, 4 and 6 were tested using both undersampling patterns.

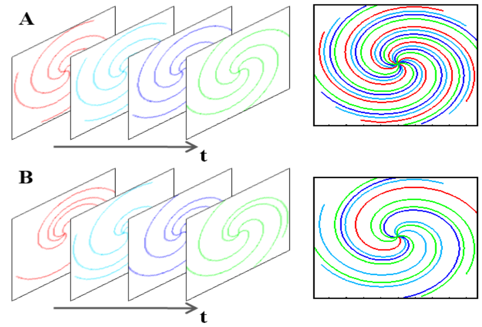

Fig. 1. Uniform rotation (top A) and random (bottom B) undersampling patterns. Four consecutive frames are shown on the left and the composite of these four frames are shown on the right. For a period during the scan, uniform rotation sampling covers a larger area of *k*-space than the random sampling pattern.

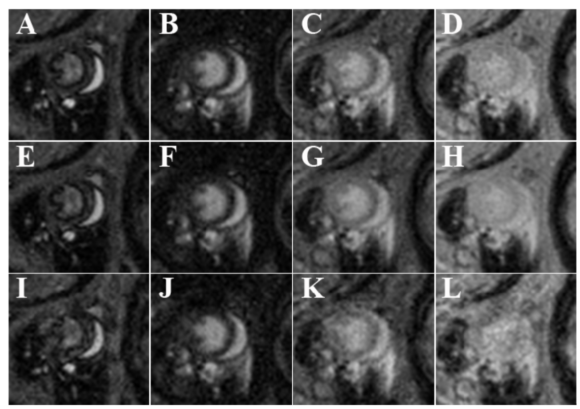

Fig. 2. CS reconstructed images example. A-D are fully sampled images. E-H are images from acceleration rate 2 and uniform rotation pattern undersampled k-space. I-L are images from rate 2 and random pattern undersampled k-space. Four columns represent four different TIs.

Results: Excellent image quality was obtained for CS multi-TI spiral images, as illustrated in Fig. 2, where rate-2 CS accelerated images (Fig. 2, E-H) appear nearly identical to fully sampled images that underwent conventional reconstruction (Fig. 2, A-D). In the examination of different undersampling patterns, better image quality was consistently obtained using the uniform rotation pattern as compared to randomly selected interleaves. This finding is illustrated in Fig. 2, where fully sampled images at four different TIs are shown in the top row (A-D), rate-2 accelerated images using the uniform rotation pattern are shown in the middle row (E-H), and rate-2 accelerated images using random interleaves are shown in the bottom row (I-L). This finding is reiterated in Fig. 3, where mean squared error (MSE) results show that the uniform rotation method has lower MSE than random interleaves. MSE results also illustrate greater error for higher acceleration rates.

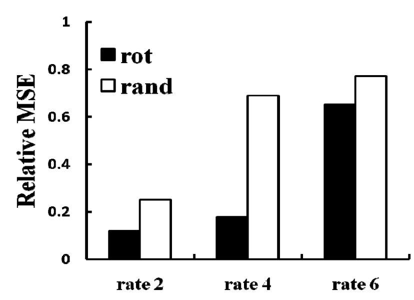

Fig. 3. Image reconstruction errors of rate 2, 4 and 6 from uniform rotation and random patterns. Errors are calculated as relative MSE to fully sampled images.

Conclusions: CS for accelerated spiral MRI of multi-TI Look-Locker MRI was investigated. Temporal sparsity was incorporated into a constrained nonlinear iterative reconstruction algorithm. A sampling pattern employing rotations of angularly-uniformly spaced interleaves provided better image quality compared to randomly selected interleaves. Rate-2 acceleration led to excellent image quality, with artifacts becoming more prominent at higher acceleration rates. Future work will investigate using variable density spirals to achieve full sampling at the center of *k*-space with undersampling at higher spatial frequencies. This approach may be lead to better image quality at higher acceleration rates. CS shows promise for achieving at least rate 2 acceleration of multi-TI spiral images for use in multi-TI ASL.

References: [1] Doneva et al. MRM 2010 64:1114-1120. [2] Fessler. IEEE T-SP 2003 (Feb) 51(2):560-74. [3] Vandsburger et al., MRM 2010 63:648–657. [4] Adluru et al. MRM 2007 57:1027-1036. [5] Lustig et al. MRM 2007 58:1182-1195.

Acknowledgements: This work was funded in part by Siemens Medical Solutions.